Asian Journal of Nanoscience and Materials 4 (2021) 188-200

SPC

Asian Journal of Nanoscience and Materials

Journal homepage: www.ajnanomat.com

Original Research Article

Hydrothermal synthesis of ZnO nanoparticles and comparison of its adsorption characteristics with the natural adsorbent (mango peel)

Elnaz Rezaei-Aghdam, Ali Shamel, Mohammad Khodadadi-Moghaddam, Gholamreza Ebrahimzadeh Rajaei*, Sahar Mohajeri

Department of Chemistry, Ardabil Branch, Islamic Azad University, Ardabil, Iran

ARTICLE INFORMATION

Received: 14 February 2021
Received in revised: 13 March 2021
Accepted: 21 March 2021
Available online: 17 May 2021

DOI: 10.26655/AJNANOMAT.2021.3.2

KEYWORDS

Adsorption
Blue 221
Dye removal
Zinc oxide nanoparticles
Mango peel

ABSTRACT

This study focuses on the utilization of ZnO (as synthetic) and mango peel (natural adsorbent) to remove blue 221 dye from aqueous solutions. First, ZnO nanoparticles (NPs) were synthesized and detected using the descriptor-based techniques, including scanning electron microscopy (SEM), transmission electron microscopy (TEM), Fourier-transform infrared spectroscopy (FTIR), N_2 adsorption/desorption isotherms (BET), and X-ray diffraction (XRD). Various operational parameters including adsorbent concentration, pH, adsorbent dose, contact time, and stirring speed were investigated. The obtained kinetic results demonstrated great compatibility of the pseudo-second-order model with the experimental data. The effects of thermodynamic parameters were calculated to confirm the endothermic, spontaneous and physical nature of adsorption process. Langmuir and Freundlich isotherm models were utilized to fit the obtained equilibrium data. Freundlich model was found sufficient to explain the adsorption of blue 221 dye by ZnO NPs and mango peel. The results indicated that the ZnO NPs performed better in blue 221 dye removal as compared with mango peel. The mean size of ZnO NPs was found to be 22.16 nm. The specific surface area of ZnO NPs was obtained 26.85 $m^2.g^{-1}$ and pore volume and pore-size were 0.0581 $cm^3.g^{-1}$ and 1.22 nm, respectively. The maximum adsorption capacity of blue 221 dye on ZnO NPs and mango peel was estimated as 133.33 and 476.19 $mg.g^{-1}$, respectively.

Corresponding author, email: farzad_rajaei@yahoo.com (Gh. Ebrahimzadeh Rajaei).
Tel.: +09845 33728020.

Graphical Abstract

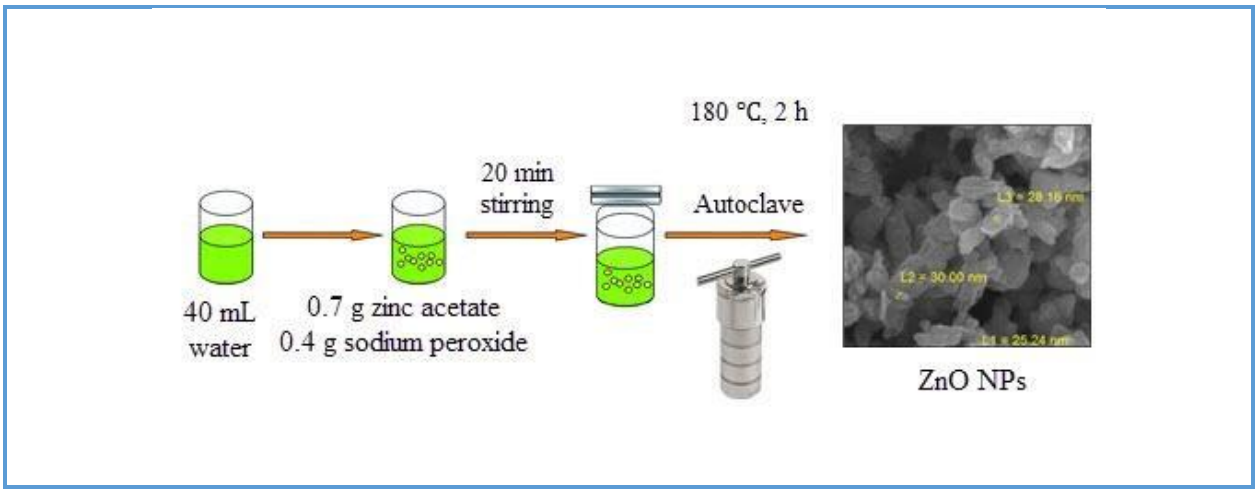

Introduction

As one of the prominent elements of nature, water is exposed to numerous pollutions. Among the various pollutants, dyes and aromatic compounds, and the toxic heavy metals cations, are destructive and non-biodegradable [1–3]. Some research studies reported that dyes are one of the most hazardous chemicals in industrial wastewaters [4, 5]. Based on literature, dyes are organic materials with complex structure, often toxic, carcinogenic, and non-biodegradable [6, 7]. Among different types of dyes, the removal of the reactive dyes in the textile industry is more important. Reactive dyes are sulfonated and highly soluble in water and do not decompose under aerobic conditions [8]. Due to their azo structures which containing one or more -N=N- bonds connected to aromatic chains, their destruction is difficult which may challenge wastewaters' filtration methods. Long-term exposure to dyes can result in skin allergies, irritation, genetic mutations, and cancer [9–11].

Various methods have been developed for removing of dyes from wastewaters including; coagulation and clotting, physical and chemical-biological treatments, chemical oxidations, electrochemical technique, ion exchange, surface adsorption, and synthetic processes including ozonation-coagulation and clotting–ion exchange [12–15]. A highly efficient method for removing of various dyes from industrial wastewater is the surface adsorption process, as these compounds can be simply transferred into the solid phase [16]. On the other hand, the used adsorbents can be recovered and then reused in the process or collected and dried without direct contact with the environment. Also, it has been proved that the adsorption process to be a suitable wastewater treatment method due to its low investment cost, ease of design, and use of non-toxic compounds [17].

Among the different types of synthetic adsorbents, the use of nanosorbents is more important due to the many capabilities of nanotechnology in the removal and control of environmental pollution and treatment [18–21]. Among the reasons that have distinguished the use of nanoparticles to remove environmental pollutants in recent years are low volume compared to other adsorbents, easy recycling of adsorbents, less sludge production, very high selectivity, and ability to produce cheap adsorbent nanoparticles [11, 22]. Today, among the various nanosorbents, metal nanoparticles with different morphologies are

more evident, especially those used in water treatment systems. These nanoparticles include such as titanium oxide, aluminum oxide and zinc oxide [23].

Nowadays, zinc oxide nanoparticles are widely used as an environmentally friendly material due to their many properties. High chemical stability, superior adhesion and coating capability, excellent catalytic properties, recoverability, UV absorption and most importantly, non-toxic antibacterial and antiseptic ability for pathogenic effects on humans are among these key features. Therefore, these good properties make zinc oxide NPs widely used in various fields [24–26].

There are different methods for the synthesis of nano zinc oxide, such as sol-gel, hydrothermal, and sonochemical [23, 27]. In this work, the hydrothermal technique was used. The advantages of this method are including the high efficiency, optimal control capability, easy method, product materials with uniform size distribution, less energy consumption, and less damage to the environment [28].

For the adsorption process, the cost of the adsorbent is one of the most important factors [29, 30]. Therefore, the application of low-cost and environmentally-friendly natural adsorbents could be an interesting approach. Natural sorbents, on the other hand, have no environmental consequences [31, 32]. In this study, the dried peel of mango was employed as a natural adsorbent.

The main objective of the present study is to remove blue 221 dye from aqueous solution through ZnO NPs and mango peel and to determine their kinetics and isothermal models under optimal conditions (pH, adsorbent dose, contact time, and dye concentration).

Experimental

Materials & methods

In this study, blue 221 dye with the molecular formula of $C_{33}H_{24}ClCuN_9Na_3O_{15}S_4$ and molecular weight of 1082.83 g/mol was purchased. The use of this dye is common in the textile industry. It was provided through Fluka Company 98%.

Hydrochloric acid (HCl), sodium hydroxide (NaOH), zinc acetate-dihydrate ($C_4H_6O_4Zn$, $2H_2O$), sodium peroxide (Na_2O_2), powder and dried of mango peel were also used. In this study, twice distilled water was applied for preparing all solutions and reagents. All reagents and chemicals were in analytical grade (purity>99%).

Also, a 781 pH/Ion Meter pH meter manufactured by Metrohm, Herisau Switzerland, a XPS 120-31 model ultrasonic-cleanerPercellys24 BER300P24 homogenizer, a Compact Shaker KS15 shaker, a Teflon lined steel Autoclave (AUTO-PTFE, SAFE TEMP–200 °C), and Pekin Elmer Lamba25 UV-Vis spectrophotometer were used in this study.

Syntheses of ZnO nanoparticles

The ZnO nanoparticles were prepared through the hydrothermal method [33]. 0.7 g zinc acetate dihydrate was mixed with 0.4 g sodium peroxide followed by adding 40 mL distilled water and 20 min of stirring. The mixture was then transferred into an autoclave at 180 ℃ for 2 h. When it was cooled to the room temperature, the ZnO nanoparticles were centrifuged and dried after washing with water and ethanol.

Adsorption

Optimization of operational parameters

pH, adsorbent dose, contact time, the concentration of blue 221 dye, and stirring speed were optimized to achieve a high adsorption capacity.

Through a stock solution of blue 221 with concentration of 100 mg.L^{-1}, other solutions with different concentrations (from 10 to 100 at 10 mg.L^{-1} intervals) were provided to obtain the optimal adsorbent concentration. The best pH was determined by testing the process at different pH values (2-10), with a blue 221 dye concentration of 100 mg.L^{-1}. The adjustment of pH was performed with the addition of NaOH (0.1 M) or HCl (0.1 M), and using a pH Meter. About 0.02 g of adsorbents were added to the solutions; the solution was then mixed by a magnetic stirrer at 150 rpm and temperature of 25 ℃ for 10 min. The solutions were then smoothed and centrifuged. The adsorption ratio of the final solution was measured by a spectrophotometer at 610 nm.

In all the experiments, the following equations were used [34]:

$$q_e = \frac{(C_0 - C_e) \times V}{W} \quad (1)$$

$$q_t = \frac{(C_0 - C_t) \times V}{W} \quad (2)$$

in which q_e (mg.g^{-1}) indicates the quantity of adsorbed substance at equilibrium time, C_e represents dye equilibrium concentration in terms of mg.L^{-1}, C_0 (mg.L^{-1}) denotes the dye initial concentration in liquid phase, q_t (mg.g^{-1}) shows the quantity of the adsorbed material at time t, C_t (mg.L^{-1}) represents the concentration in the liquid phase at any given time, V (L) and W (g) are related to the solution volume and amount of used adsorbent, respectively.

Kinetics of adsorption

To study the kinetics of the reaction, 25 mL of blue 221 solutions with an initial concentration of 100 mg.L^{-1} was infused in different beakers. The solution pH was adjusted to 2, followed by adding 0.02 g of adsorbent. Samples were mixed for different periods of time (1-90 min; 5-min interval for the first 30 min and 10-min intervals for the rest of reaction duration) by a magnetic stirring at an optimal speed of 150 rpm. After smoothing, centrifugation, and sampling, a UV-Vis spectrophotometer was employed to record the sample optical absorption at 610 nm. The adsorption kinetics was explored by fitting the obtained data into the kinetic models.

Temperature effect

25 mL of blue 221 solutions with an initial concentration of 100 mg.L^{-1} was prepared for assessing the effect of temperature. The solutions pH was set to 2 followed by adding 0.02 g of adsorbents. The solutions were then mixed at different temperatures of 25, 35, 45, and 55 ℃ for a specific period of time by a magnetic stirrer at the optimal speed of 150 rpm. After smoothing, centrifuge of the solutions, and sampling, their final absorbance was measured by a spectrophotometer. The equilibrium concentrations (C_e) were calculated according to the obtained data, and thermodynamic parameters were determined.

Adsorption isotherm

25 mL of Blue 221 dye solutions with different concentrations of 25, 50, 75, 100, 125, and 150 mg.L^{-1} were prepared at the pH of 2, then 0.02 g of adsorbents was added to each case. The reaction continued at different temperatures from 25 to 55 ℃ at 10-degree intervals under magnetic stirring at an optimal speed of 150 rpm. After sampling, the absorbance of the solutions was measured by a spectrophotometer. The isotherms were determined according to the obtained data.

Results and Discussion

Characterization

XRD pattern of ZnO NPs (Figure 1) showed 9 peaks at 2θ equal to 31.78, 34.43, 36.28, 47.59,

56.63, 62.85, 67.94, 69.01, and 69.09^0 corresponding with (100), (002), (101), (102), (110), (103), (200), (112), and (201) planes, respectively [33–35]. These peaks indicated that the synthesized structure was hexagonal. The diffraction peaks were following to the standard card no. of (JCPDS card number 79-0205).

Based on the Scherer equation, it is possible to approximate the crystallite size, D, according of the following equation:

$$D = (0.9\times\lambda) / (\beta \cos\theta) \quad (3)$$

in which, β indicates the full width at half maximum (FWHM), θ is the Brag angle and λ denotes the wavelength. The most intense peak was considered to determine the FWHM. The mean size of the nanoparticles was 22.16 nm [36–38].

As a result of BET (Brunauer–Emmett–Teller) theory, the diagram of N_2 adsorption and desorption of the sample in Figure 2 illustrates that this sample contains meso cavities in its structure. Using the information obtained from the diagram, a cylindrical geometric shape was determined for the structure of the cavities. The specific surface area of ZnO NPs was obtained 26.85 $m^2.g^{-1}$ and pore volume and pore-size were 0.0581 $cm^3.g^{-1}$ and 1.22 nm, respectively. The small pore-size and the specific surface area of ZnO NPs indicate the synthesis of nanoparticles, which makes this suitable special surface for adsorption of blue 221 dye from aqueous solutions [33, 39-40].

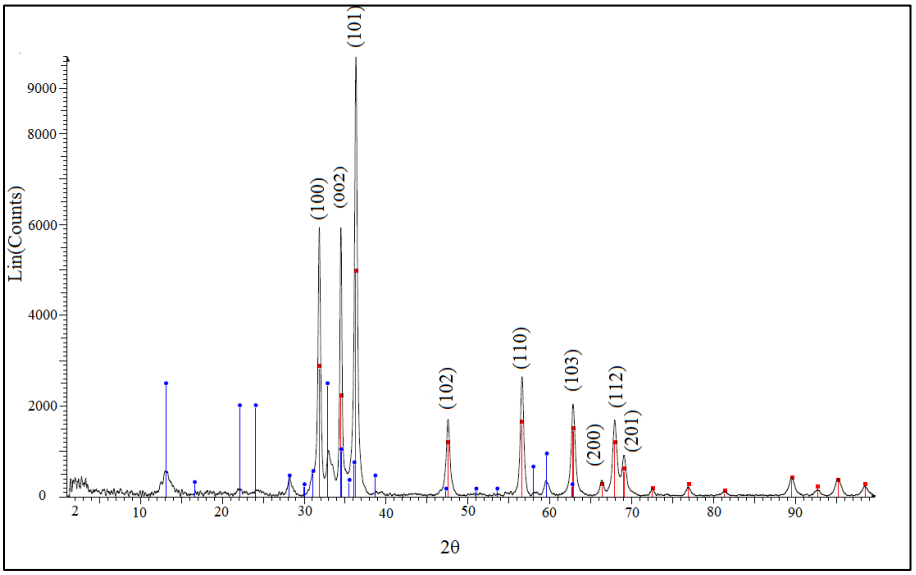

Figure 1. XRD pattern of ZnO NPs synthesized using hydrothermal method

In the FT-IR spectra (Figure 3**a**), the peaks at 3378.79 and 1388 cm^{-1} could be caused by the stretching vibrations of O-H; while the stretching vibration of Zn-O can lead to the appearance of peaks at 1510.12 and below 1000 cm^{-1}, and also can be assigned to the stretching vibrations of Zn-O [33, 35, 41]. FT-IR results of the natural adsorbent (mango peel) (Figure 3**b**) revealed that the peak at 1000-1500 cm^{-1} can be due to the lignin compounds; whereas those peaks appearance at 1500-2000 cm^{-1} can be due to the carboxyl groups, protein, and water. The peaks at the range of 2000 to 2500 cm^{-1} also suggest the existence of ester and those appearing at 3000-3500 cm^{-1} can be due to the presence of polysaccharides and water [42].

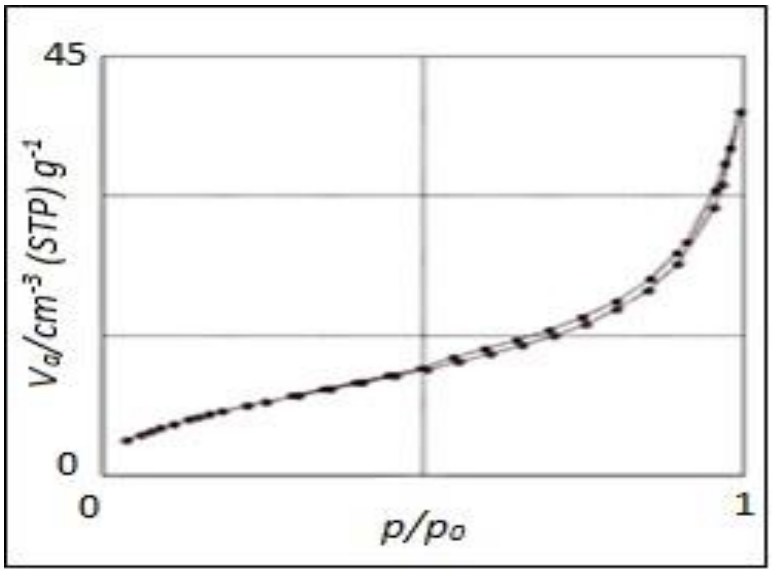

Figure 2. N_2 adsorption and desorption diagram at 77 K for ZnO NPs synthesized using hydrothermal method

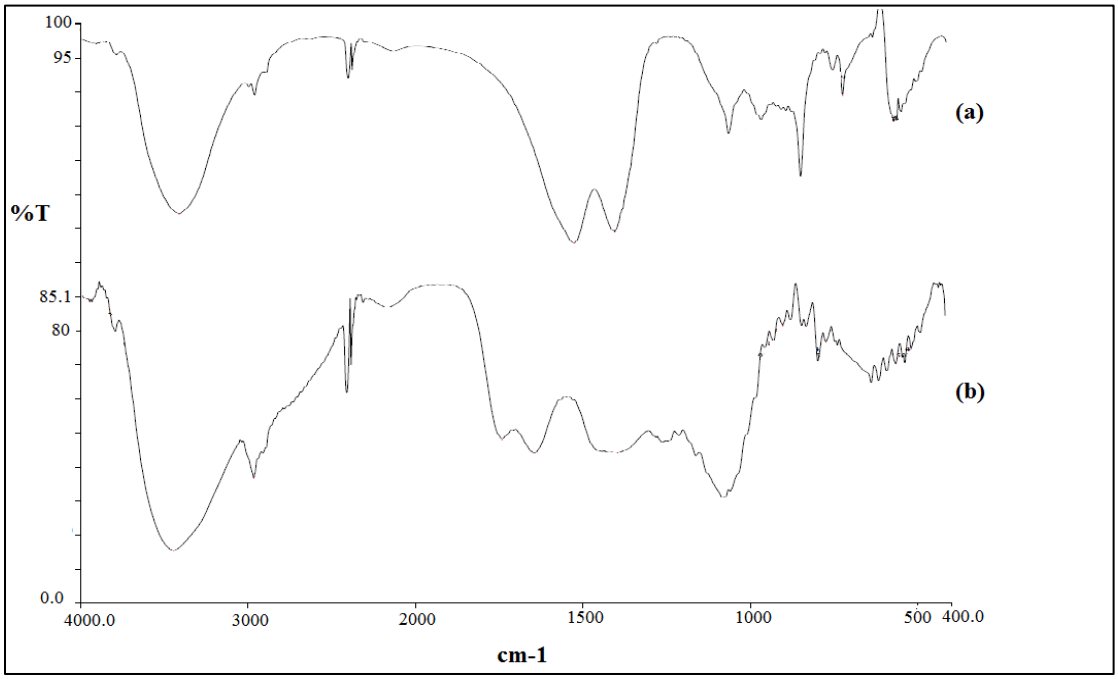

Figure 3. FT-IR spectra for a) ZnO NPs synthesized hydrothermal method, and b) mango peel

SEM image (Figure 4**a**) of ZnO NPs synthesized through hydrothermal method shows a needle-shaped structure with hexagonal and spherical structures. The mean size of the nanoparticles was 28.16 nm and their distribution extended in the range of 25-40 nm [33–35]. The TEM results (Figure 4**b**) also show the distribution of ZnO nanoparticles throughout the sample.

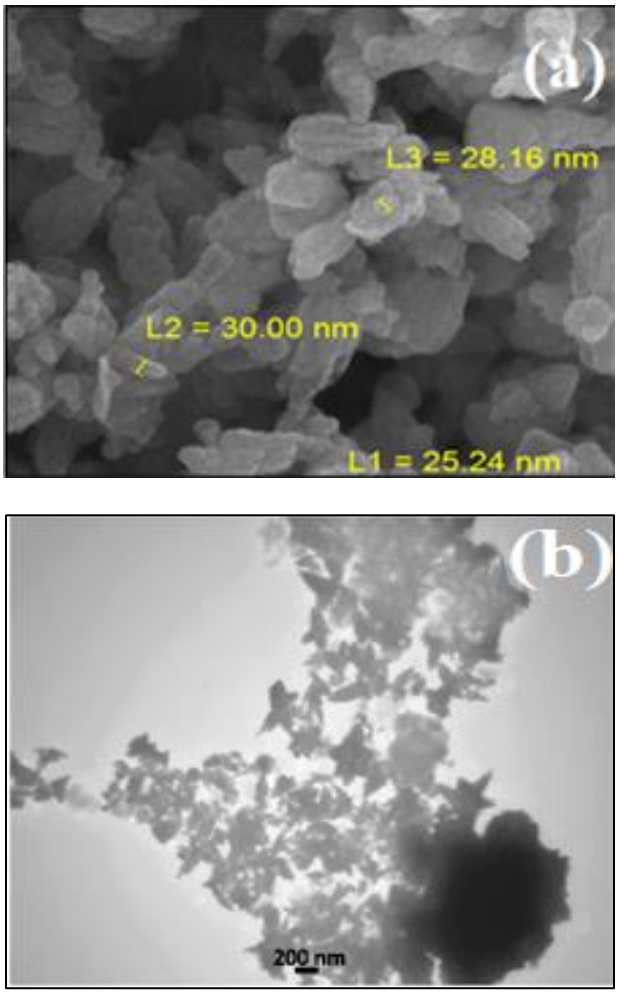

Figure 4. a) SEM and b) TEM images of ZnO NPs synthesized through hydrothermal method

Optimization of operational parameters

The results showed that the best concentration of blue 221 dye was 100 $mg.L^{-1}$ for all the experiments. pH optimization demonstrated that high capacities of blue 221 dye adsorption can be achieved at pH of 2 using ZnO NPs and mango peel. Since the colored pollutant of blue 221 is an anionic dye, the adsorbent surface must be positively-charged to achieve optimal adsorption, which was evidenced by the acquired data. Other optimization results are as follows: adsorbent dose= 0.02 g, contact time= 10 min, and stirring speed= 150 rpm.

Kinetics of adsorption

The occurrence of penetration from the inner part of a layer according to the solid capacity can be understood from pseudo-first-order kinetic model. Unoccupied sites of the adsorbent surfaces are associated with the variations in the adsorption by time. The pseudo-second-order kinetic model states that chemical adsorption is a step for reducing the speed and can control the surface adsorbing process via the solid phase in which the adsorption rate is proportional to the square of the number of unoccupied sites. Following formulas show common forms of the first- and second-order kinetics [43]:

$$\ln(q_e - q_t) = \ln q_e - k_1 \cdot t \quad (4)$$

$$\left(\frac{t}{q_t}\right) = \left(\frac{1}{k_2 \cdot q_e^2}\right) + \left(\frac{1}{q_e}\right) \cdot t \quad (5)$$

in which q_e (mg.g^{-1}) and q_t (mg.g^{-1}) indicate the adsorbed dye equilibrium quantity, and the adsorbed dye quantity at time t, respectively. Also, k_1 (min^{-1}) and k_2 (g.mg^{-1}.min^{-1}) represent the equilibrium pseudo-first-order and pseudo-second-order kinetic rate constants, respectively. By calculating the correlation coefficients, the level of conformity with these kinetic models can be determined.

Table 1 and Figure 5 represent the information about the kinetic data for the pseudo-first and second-order kinetics. The high correlation coefficient of the pseudo-second-order diagram indicates that this equation can well describe the kinetics of blue 221 dye adsorption onto the used adsorbents.

For comparison, data reported by Chih-Wei Chiu and *et al.*, which used α-chitosan as an adsorbent to remove 221 blue dye and the data obtained by Levent Gürel, which used capia pepper to remove the 221 blue dye, are also represented in Table 1 [44-45]. Due to the high values of qe for both adsorbents used in this study, it shows that both adsorbents were suitable for removing 221 blue dye.

A comparison of the blue 221 dye removal percentages showed that ZnO nanoparticles are better adsorbents compared to the mango peel, as seen in Figure 6.

Table 1. Kinetic parameters obtained from adsorption of blue 221 dye on ZnO NPs and mango peel surfaces

Samples	Pseudo-first-order kinetic model			Pseudo-second-order kinetic model		
	k_1 (min^{-1})	q_e (mg.g^{-1})	R^2	k_2 (g.mg^{-1}.min^{-1})	q_e (mg.g^{-1})	R^2
ZnO NPs	1.00×10^{-4}	2.716	0.9112	0.0165	108.69	0.9999
Mango peel	8.00×10^{-5}	2.717	0.9609	0.0210	106.38	0.9999
α-chitosan [44]	-	0.9800	0.9796	1.657	96.150	0.9981
pepper seeds [45]	1.18×10^{-3}	57.80	0.9800	8.330×10^{-5}	97.090	0.9900

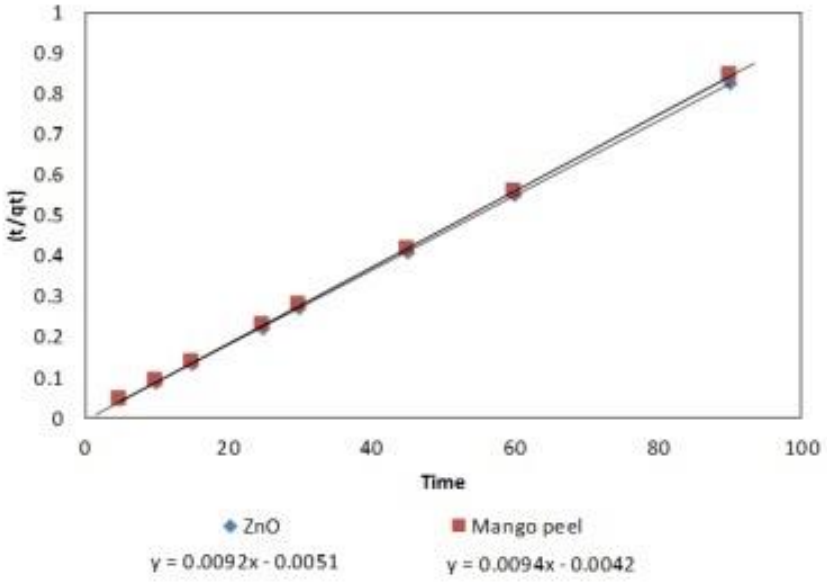

Figure 5. The pseudo-second-order kinetic model for adsorption of blue 221 dye on ZnO and mango peel

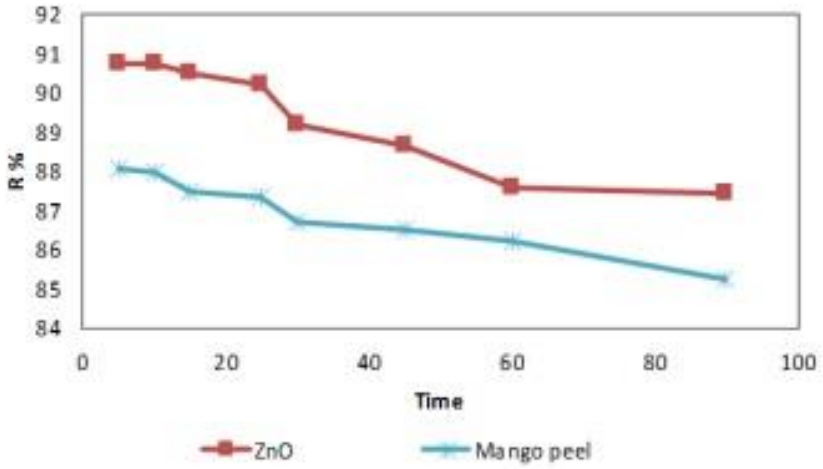

Figure 6. Blue 221 dye removal percentages as a function of time (min) for ZnO NPs and mango peel adsorbents

Temperature effect

Temperature is a key and essential factor in thermodynamics studies. The most important aspect of the laws of thermodynamics is that they can theoretically predict the chemical reaction under certain conditions.

The following equations can be used to calculate of thermodynamic parameters such as Gibbs free energy changes, enthalpy, as well as entropy [44]:

$$K_C = \frac{C_S}{C_e} \quad (6)$$

$$\Delta G° = -RT\ ln\ K_C \quad (7)$$

$$ln\ K_C = \left(\frac{\Delta S°}{R}\right) - \left(\frac{\Delta H°}{RT}\right) \quad (8)$$

Where K_c is an equilibrium constant, C_s ($mg.dm^{-3}$) is adsorbed concentration on the adsorbent surface at equilibrium time, C_e ($mg.dm^{-3}$) is dye equilibrium concentration in solution, T (K) is solution temperature, and R ($J.mol^{-1}.K^{-1}$) is universal gas constant. The obtained results were summarized in Table 2.

It can be understood from the findings of the thermodynamic parameters that adsorption of blue 221 dye on ZnO NPs and mango peel surfaces is endothermic and spontaneous. Also, according to the enthalpy change's values, the adsorption of blue 221 dye on ZnO NPs and mango peel surfaces is physical.

Table 2. Thermodynamic parameters of blue 221 adsorption on ZnO NPs and mango peel, calculated using Vant-Hoff equations

Samples	T (K)	C_e ($mg.dm^{-3}$)	C_s ($mg.dm^{-3}$)	K_c	ΔG° (kJ/mole)	ΔS° (kJ/mole K)	ΔH° (kJ/mole)
ZnO	298.15	9.22	90.77	9.83	-5.66	0.099	24.08
	308.15	7.69	92.30	12.00	-6.36		
	318.15	6.43	93.56	14.54	-7.08		
	328.15	3.85	96.14	24.95	-8.77		
Mango peel	298.15	8.89	91.10	10.23	-5.76	0.096	23.24
	308.15	8.16	91.83	11.25	-6.20		
	318.15	7.05	92.94	13.16	-6.81		
	328.15	3.77	96.22	25.51	-8.83		

Adsorption isotherm

Adsorption isotherm represents the distribution of soluble material between solution and adsorbent surface. Langmuir model assumes that the adsorption takes place in some special homogenous sites inside of the adsorbent. Freundlich model presumes that the adsorption process occurs at the heterogeneous surfaces where adsorption heat is distributed unsteadily on the surface. The linear forms of the two models (Freundlich & Langmuir isotherm models) are [46–49]:

$$\frac{C_e}{q_e} = \left(\frac{1}{K_L Q_m}\right) + \frac{C_e}{Q_m} \quad (9)$$

$$log\ q_e = log\ K_F + \left(\frac{1}{n}\right) log\ C_e \quad (10)$$

Where q_e is amount of adsorbed material at equilibrium, C_e shows the solution concentration at equilibrium, K_L is an equilibrium constant, Q_m denotes the highest capacity of adsorption, K_F and n are constants for a given adsorbate and adsorbent at a given temperature.

The results obtained from thermodynamic studies were showed in Table 3 and Figure 7. The isothermal diagrams and correlation coefficients of lines indicate that the Freundlich model is the best isotherm model for adsorption of blue 221 dye on ZnO NPs and mango peel surface. The data obtained by Ali H. Jawad *et al.*, which used pomegranate peel to remove methylene blue dye [50], were compared with the data of our study.

Table 3. Isotherm parameters for adsorption of blue 221 dye on ZnO NPs and mango peel surface

Samples	Langmuir Isotherm			Freundlich Isotherm			
	Q_m (mg/g)	K_L (L/mg)	R^2	1/n	n	K_F	R^2
ZnO NPs	133.33	0.049	0.9092	1.56	0.64	3.69	0.9993
Mango peel	476.19	0.033	0.9558	0.83	1.20	17.18	0.9947
pomegranate peel [50]	200.00	0.050	0.9890	0.32	3.25	35.60	0.9740

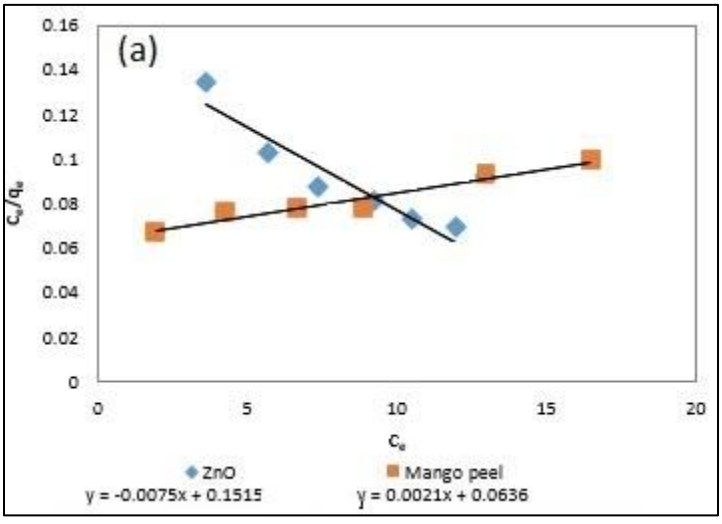

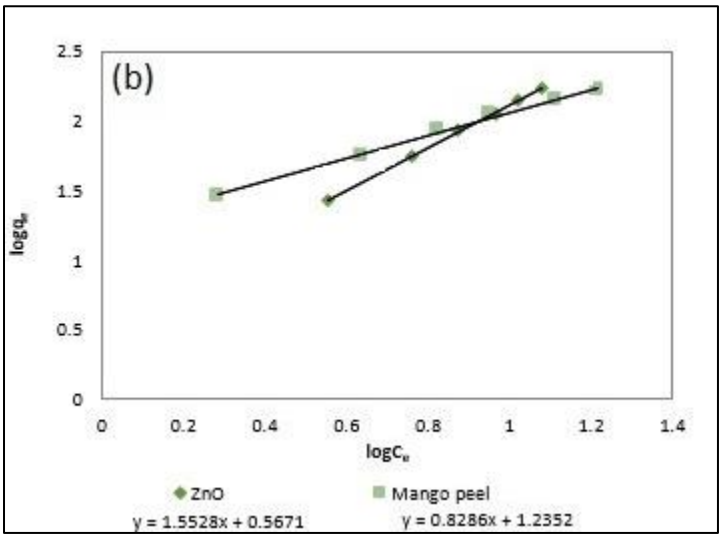

Figure 7. The isotherms of blue 221 adsorption on ZnO NPs and mango peel surface: a) Langmuir and b) Freundlich models

Conclusions

This research study investigated the removal of blue 221 dye from aqueous solutions by various adsorbents (ZnO NPs and mango peels). In the first step, the effects of operational parameters were studied. According to our findings, the best concentration of blue 221 dye in all experiments was 100 $mg.L^{-1}$. Other optimized parameters are: adsorbent dose = 0.02 g, contact time = 10 min, stirring speed = 150 rpm, and pH = 2. Various kinetic models were studied. The obtained results illustrated that the pseudo-second-order kinetic model is the most appropriate method for the removing of blue 221 dye by ZnO NPs and mango peel. Thermodynamic parameters also revealed that adsorption of blue 221 dye was endothermic and spontaneous. According to the enthalpy change's values, adsorption process was physical. Study of the isotherm models revealed that Freundlich model is the preferable isotherm model to describe blue 221 dye adsorption on ZnO NPs and mango peel surface. The results showed that ZnO NP had a better performance in removing blue 221 dye than mango peel.

Acknowledgments

The authors would like to appreciate the Islamic Azad University of Ardabil for providing all the necessary facilities for conducting the experiments.

Disclosure Statement

No potential conflict of interest was reported by the authors.

Orcid

Ebrahimzadeh Rajaei 0000-0002-6787-5472

References

[1]. Hosseini M., Nabavi S.M.B., Nabavi S.N., Pour N.A. *Environmental Monitoring and Assessment,* 2015, **187**:1

[2]. Pathania D., Sharma S., Singh P. *Arabian Journal of Chemistry*, 2017, **10**:S1445

[3]. Ajormal F., Moradnia F., Taghavi Fardood S., Ramazani A. *Journal of Chemical Reviews*, 2020, **2**:90

[4]. Lima E.C., Royer B., Vaghetti J.C.P., Simona N.M., da Cunha B.M., Pavan F.A., Benvenutti E.V., Catalu˜na-Veses R., Airoldi C. *Journal of hazardous Materials,* 2008, **155**:536
[5]. Monash P., Pugazhenthi G. *Adsorption,* 2009, **15:**:390
[6]. Soleimani-Gorgani A., Taylor J.A. *Dyes and Pigments*, 2006, **68**:109
[7]. Tavares M.G.R., Santos D.H.S., Tavares,M.G., Duarte J.L.S., Meili L., Pimentel W.R.O., Tonholo J., Zanta C.L.P.S. *Water, Air, & Soil Pollution*, 2020, **231**:82
[8]. Ozdemir O., Armagan B., Turan M., Çelik M.S. *Dyes and Pigments*, 2004, **62**:49
[9]. Kant R., Rattan V.K. *Carbon letters*, 2010, **11**:206
[10]. Demirbas E., Nas M.Z. *Desalination*, 2009, **243**:8
[11]. Taghavi Fardood S., Forootan R., Moradnia F., Afshari Z., Ramazani A. *Materials Research Express*, 2020, **7**:015086
[12]. Abd El fatah M., Ossman M.E. *International Journal of Environmental Research*, 2014, **8**:741
[13]. Li Q., Zhao Y., Wang L., Aiqin W. *Korean Journal of Chemical Engineering*, 2011, **28:**1658
[14]. Ismail B., Tajammul S., Akram S. *Chemical Engineering Journal*, 2013, **219**:395
[15]. Sheikhshoaie I., Rezazadeh A., Ramezanpour S. *Asian Journal of Nanosciences and Materials*, 2018, **1**:271
[16]. Chen W., Zhang H., Liang Y., Ding H., Sun S. *Frontiers in Chemistry*, 2018, **6**:1
[17]. Crini G., Lichtfouse E., Wilson L., Morin-crini N., Crini G., Lichtfouse E., Wilson L. *Environmental Chemistry for a Sustainable World,* 2019,**18**:23
[18]. Sharma Y.C., Srivastava V., Singh V.K., Kaul S.N., Weng C.H. *Environmental Technology*, 2009, **30**:583
[19]. Ramazani A., Ayubi M., Moradnia F., Abdpour S. *Chemical Methodologies*, 2019, **3**:583
[20]. Moradnia F., Taghavi Fardood S., Ramazani A., Min B., Joo S.W., Varma R.S. *Journal of Cleaner Production*, 2021, **288**:125632
[21]. Saeidian H., Mirjafary Z., Abdolmaleki E., Moradnia F. *Synlett*, 2013, **24**:2127
[22]. Moradnia F., Taghavi Fardood S., Ramazani A., Gupta V.K. *Journal of Photochemistry and Photobiology A: Chemistry*, 2020, **392**:112433
[23]. Fardood S.T., Moradnia F., Mostafaei M., Afshari Z., Faramarzi S.G. *Nanochem Res*, 2019, **4**:86
[24]. Zhong Q., Huang X., Duan J., Liu J., Sun F., He X. *Materials Letters*, 2008, **62**:188
[25]. Thirumavalavan M., Huang K.L., Lee J.F. *Materials*, 2013, **6**:4198
[26]. Communication I.C., Saeidian H., Moradnia F. Quarterly *Journal of Iranian Chemical Communication*, 2017, **5**:252
[27]. Talam S., Karumuri S.R., Gunnam N. *ISRN Nanotechnology*, 2012, **2012**:1
[28]. Baruwati B., Kumar D.K., Manorama S.V. *Sensors and Actuators, B: Chemical*, 2006, **119**:676
[29]. Belviso C., Cavalcante F., Ragone P., Fiore S. *Chemosphere*, 2010, **78**:1172
[30]. Sen Gupta S., Bhattacharyya K.G. *Physical Chemistry Chemical Physics*, 2012, **14**: 6698
[31]. Khattri S.D., Singh M.K. *Indian Journal of Chemical Technology*, 1999, **6**:112
[32]. Dharmendirakumar M.G., Vijayakumar R.T., Vijayakumar G., Tamilarasan R., Dharmendirakumar M. *Journal of Materials and Environmental Science*, 2015, **3:**157
[33]. Rezaei-Aghdam E., Shamel A., Khodadadi-Moghaddam M., Ebrahimzadeh Rajaei G., Mohajeri S. *Research on Chemical Intermediates*, 2021.
[34]. Zhang C., Wei S., Hu Y., Tang H., Gao J., Yin Z., Guan Q. *Journal of Colloid and Interface Science*, 2018, **512**:55
[35]. Gharbani P., Mehalizadeh A. *Asian Journal of Nanoscience and Materials*, 2018, **2**:27

[36]. Safarkar R., Ebrahimzadeh Rajaei G., Khalili A.S. *Asian Journal of Nanoscience and Materials*, 2020, **3**:157
[37]. Taghavi Fardood S., Moradnia F., Ramazani A. *Micro & Nano Letters*, 2019, **14**:986
[38]. Moradnia F., Fardood S.T., Ramazani A., Osali S., Abdolmaleki I. *Micro and Nano Letters*, 2020, **15**:674
[39]. Li X., Lv K., Deng K., Tang J., Su R., Sun J., Chen L. *Materials Science and Engineering B: Solid-State Materials for Advanced Technology*, 2009, **158**:40
[40]. Liewhiran C., Seraphin S., Phanichphant S. *Current Applied Physics*, 2006, **6**:499
[41]. Salahuddin N.A., El-Kemary M., Ibrahim E.M. *Nanoscience and Nanotechnology*, 2015, **5**:82
[42]. Salih S.I., Oleiwi J.K., Mohamed A.S. *ARPN Journal of Engineering and Applied Sciences*, 2018, **13**:8889
[43]. Zhang N., Liu S., Jiang L., Luo M., Chi C., Ma J. *Journal of Radioanalytical and Nuclear Chemistry*, 2014, **303**:1671
[44]. Chiu C.W., Wu M.T., Lee J. C.M., Cheng T.Y. *Polymers*, 2018, **10**:1328
[45]. Gürel L. *Water Science and Technology*, 2017, **75**:1889
[46]. Jaseela P.K., Garvasis J., Joseph A. *Journal of Molecular Liquids*, 2019, **286:**583
[47]. Ebrahimzadeh Rajaei G., Khalili A.S., Fataei E., Sajadi N., Kashefi A.M. *Comptes Rendus–Chimie*, 2020, **23**:563
[48]. Ebrahimzadeh Rajaei G., Aghaie H., Zare K., Aghaie M. *Journal of Physical and Theoretical Chemistry*, 2012, **9**:137
[49]. Khalili A.S., Kashefi A.M. Sajjadi N., Fataei E., Ebrahimzadeh Rajaei G. *Biological Trace Element Research*, 2021, **199**:763
[50]. Jawad A.H., Waheeb A.S., Rashid R.A., Nawawi W.I., Yousif E. *Desalination and Water Treatment*, 2018, **105**:322

How to cite this manuscript: Elnaz Rezaei-Aghdam**,** Ali Shamel**,** Mohammad Khodadadi-Moghaddam**,** Gholamreza Ebrahimzadeh Rajaei*, Sahar Mohajeri**.** Hydrothermal synthesis of ZnO nanoparticles and comparison of its adsorption characteristics with the natural adsorbent (mango peel). *Asian Journal of Nanoscience and Materials*, 4(3) 2021, 188-200. DOI: 10.26655/AJNANOMAT.2021.3.2